Photoconductivity in *trans*-Poly(phenylacetylene) and Its Charge-Transfer Complexes

E. T. Kang,[†§] P. Ehrlich,*[†] A. P. Bhatt,[‡⊥] and W. A. Anderson[‡]

State University of New York at Buffalo, Amherst, New York 14260.
Received July 26, 1983

ABSTRACT: Steady-state and pulsed photoconductivities were explored in 4–8-μm-thick films of poly(phenylacetylene) (PPA) and PPA doped with some inorganic and organic electron-accepting compounds, particularly iodine and DDQ (2,3-dichloro-5,6-dicyano-*p*-benzoquinone). Data are reported on the dependence of the photocurrent density (J_{ph}) on the exciting wavelength (λ), the dopant concentration (Y), the light intensity (I), and the electric field (E) in *trans*-PPA. $J_{ph}(\lambda)$ shows two regions of response, one at the π–π* transition at λ <525 nm, the other in the red and near-IR in doped, as well as undoped, PPA. The latter response is associated with photodetrapping from shallow electron traps in the undoped polymer and with charge carrier generation in the charge-transfer band in the doped polymer. The field dependence is superlinear at $E \sim 10^4$–10^5 V/cm and $J_{ph} \propto I^a$, with $a \leq 0.5$. Carrier lifetimes and mobilities are reported for some conditions. Charge transport occurs by a bandlike mechanism that is modulated by shallow electron traps in the undoped polymer and by trapping in the charge-transfer complex in the doped polymer. The control of photoconductivity by the carrier recombination kinetics is an important characteristic of this semiconducting photoconductor.

Introduction

We reported recently on the presence of space charge-perturbed dark currents and photocurrents in 4–8-μm-thick films of *trans*-poly(phenylacetylene) (PPA) and PPA doped with iodine or 2,3-dichloro-5,6-dicyano-*p*-benzoquinone (DDQ). Photocurrent to dark current ratios approaching 1000 could be observed. In the undoped polymer the majority carriers were found to be electrons, injected from the negatively biased metal electrode through defect states in the band gap of the polymer, with holes being strongly trapped. Optical detrapping was shown to be responsible for the photoconductivity action spectrum that extends into the near infrared, well beyond the band edge of the polymer at about 525 nm; in PPA–I_2 and PPA–DDQ the charge-transfer complex acts as the main source and sink of charge carriers.[1,2] A screening of several different PPA preparations showed the photoconductivity to be strongly dependent on the microstructure of the polymer, such that the photosensitivity was larger in *trans*-PPA than in the cis isomer, as well as in samples of higher molecular weight.[3] This paper deals with *trans*-PPA of molecular weight 80 000, obtained in the presence of a $W(CO)_6$ catalyst.[4] The semiconductor properties[5] and dc[6] and ac conductivity[7] of *cis*-PPA and its complexes with iodine and arsenic pentafluoride were reported earlier, together with the phase equilibria between different isomers of *cis*-PPA.[8]

Experimental Section

1. Polymer Samples. The *trans*-PPA samples used in these studies had been prepared in the laboratory of Prof. Higashimura, Kyoto University, and were obtained through his courtesy. Polymerizations had been carried out in the presence of a $W(CO)_6$ catalyst in CCl_4 solution under irradiation by a high-pressure mercury lamp, yielding room-temperature-soluble *trans*-PPA of molecular weight 80 000, as measured by osmometry.[4] Films for all studies on undoped PPA and PPA–I_2 were obtained from the same polymer preparation, on PPA–DDQ from another. The photoconductivity action spectra of undoped films cast from these two different polymer preparations were identical.

2. Preparation of Photoconductive Films. Doped films were prepared by mixing dilute solutions of PPA and dopant, in chloroform or toluene, followed by pouring of the mixture over a NESA (SnO_2) or metal-coated glass slide and allowing the solvent to evaporate.[1,5] The procedure was the same for undoped films, except for omission of the mixing step. The film thickness was determined by weighing. It ranged from 4 to 8 μm and was determined to an accuracy and uniformity of ±10%. The semitransparent top electrode, which was 100–150 Å thick and 0.04–2 cm^2 in area, was then deposited on top of the PPA film in a vacuum evaporator. The top electrode was usually Pd, but sometimes Cu, Al, or Cr; the same results were obtained in each case. A thicker layer of Al, but of much smaller area, was usually deposited on the top electrode to facilitate anchoring of the lead-in wire. In this manner, the film samples were always in a diodelike or sandwich configuration of type metal/PPA/metal or metal/PPA/SnO_2. For further details, see ref 3.

3. Photoconductivity Measurements. The experimental arrangement is shown in Figure 1. The light source for the steady-state studies was a Schoeffel 150-W xenon arc gas discharge lamp (Model L-124) with a Schoeffel LPS 251 HR power supply, which was calibrated against a standard test silicon solar cell (NASA Standard) under AM 1 conditions. The spectral content of the light source was controlled by 10-nm-wide band-pass filters (Oriel Corp.) and various cutoff and neutral-density filters (Ealing Optics), whose spectral characteristics and transmittances had been determined spectrophotometrically. Both front illumination and back illumination were used. The voltage source was a dc Hewlett-Packard Model 6216 A power supply, which could put a positive or negative bias on the top electrode. Currents were fed into an FET converter–amplifier circuit and displayed on a Tektronix Model 466 storage oscilloscope.

In the transient measurements, the continuous source was replaced by a Xenon Corp. Model 457 micropulser of about 3-μs bandwidth. Depending on the choice of the measuring resistor, R, measurements could be carried out either in the voltage or in the charge accumulation mode ($RC \gg t_T$) or in the differential or current mode ($t_T \gg RC$), where C is the sample capacitance and t_T the transit time.

The field-dependent quantum yield, which must be calculated for cases where carriers are injected from the electrodes and where they are generated in the bulk of the sample, is obtained from the expression

$$Q = \frac{J_{ph}}{e\phi(1 - T)}$$

where J_{ph} is the photocurrent density, e is the electronic charge, T is the fractional transmittance of the sample, and ϕ is the photon flux.

4. UV–Visible Absorption Spectra. Film as well as solution spectra of doped and undoped PPA were determined in this study. Solution spectra were measured in standard 1-cm path-length quartz cells, and film spectra on thin films supported on glass

---

[†] Department of Chemical Engineering.

[‡] Department of Electrical and Computer Engineering.

[§] Present address: Department of Chemical Engineering, University of Singapore, Singapore 0511.

[⊥] Present address: Varian Associates, Beverly, MA 01915.

0024-9297/84/2217-1020$01.50/0

Table I
Extinction Coefficients and Equilibrium Constants of PPA-I_2 and PPA-DDQ CT Complexes at λ = 750 nm

		PPA-I_2		PPA-DDQ	
polymerization catalyst	isomeric structure	ϵ_{AD}, L/(mol·cm)	K_{eq}, L/mol	ϵ_{AD}, L/(mol·cm)	K_{eq}, L/mol
$W(CO)_6$	trans rich (ref 4)	2.6 × 10^3	46	3.3 × 10^3	110
$MoCl_5$	cis rich (ref 22)	1.2 × 10^3	77	2.4 × 10^3	220
$Fe(OAcAc)_3/Al(C_2H_5)_3$	cis rich (ref 8)	1.2 × 10^3	60	1.3 × 10^3	220

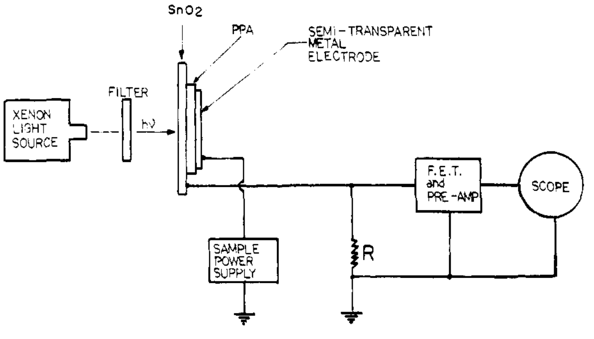

Figure 1. Experimental arrangement for photoconductivity studies.

slides, using a blank slide as reference. All measurements were carried out on a GCA/McPherson, Eu-700 series, double-beam scanning spectrophotometer, equipped with recorder and digital controller, or on a Guildford Instruments Model 250 single-beam spectrophotometer.

Results

The photoconductivity action spectra and quantum yields for undoped *trans*-PPA, as well as for PPA-I_2 and PPA-DDQ, are shown in Figures 2 and 3. These figures show the long wavelength tail of the photoconductivity band associated with the π-π^* transition, as well as another band that extends well into the near-infrared.[9] In undoped PPA, this band results from the photodetrapping of shallow traps below the conduction band (see Discussion), in the doped polymers it parallels the charge-transfer band throughout the region over which measurements could be made. The entire charge-transfer band was traced by Kuwane et al. in PPA-DDQ,[10] who located the maximum of this very broad absorption at about 940 nm. The correspondence between the charge-transfer bands of the doped polymers and their photoconductivity spectra points to the charge-transfer complex (CTC) as source of the photocarriers; presumably that complex also accounts for the dark conductivity of PPA-I_2 and PPA-AsF_5. The latter complex is only marginally photoconductive.[3]

The charge-transfer interaction of PPA with iodine is quite complex, involves several species with different stoichiometry,[9,11] and will be reported on separately.[12] The simplest complex—that with 1:1 stoichiometry—is susceptible to a Benesi-Hildebrand analysis, as is PPA-DDQ. Equilibrium constants, K_{eq}, and extinction coefficients, ϵ_{AD}, differ for different PPA isomers, but the magnitudes of K_{eq} all show a strong tendency toward complex formation (Table I). It should be noted that the charge-transfer complex has also been shown to play a key role in the dark conductivity of halogen-doped polyacetylene.[13]

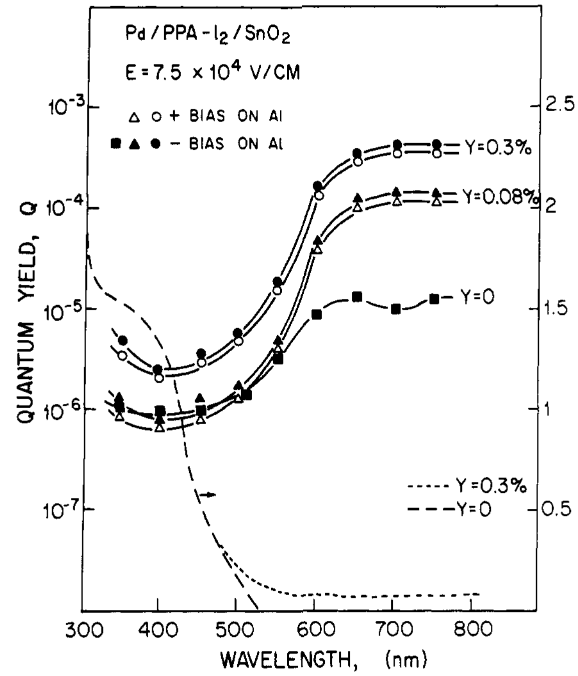

Figure 2. Absorbance and photoconductivity action spectra of PPA-I_2.

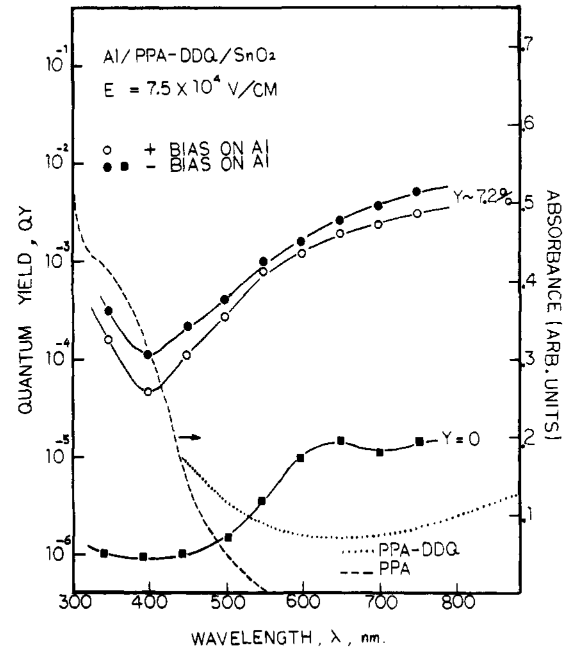

Figure 3. Absorbance and photoconductivity action spectra of PPA-DDQ.

The dependence of the photocurrent density, J_{ph}, on the doping level, Y, expressed as mol % dopant per mol monomer, is shown in Figures 4 and 5. Note that in PPA-DDQ there exists an optimum in the value of Y that is associated with a maximum value of J_{ph}; a similar maximum would probably occur in PPA-I_2 if higher doping levels were achievable without crack development in the films.

The intensity (I) dependence of J_{ph} is shown in Figure 6. The slope of the log-log plots ranges from 0.3 to 0.45

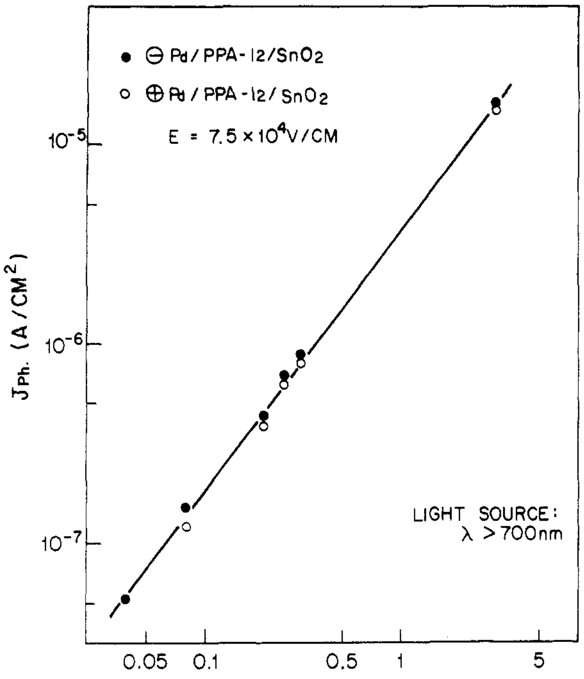

Figure 4. Photocurrent density vs. doping level in PPA-I_2.

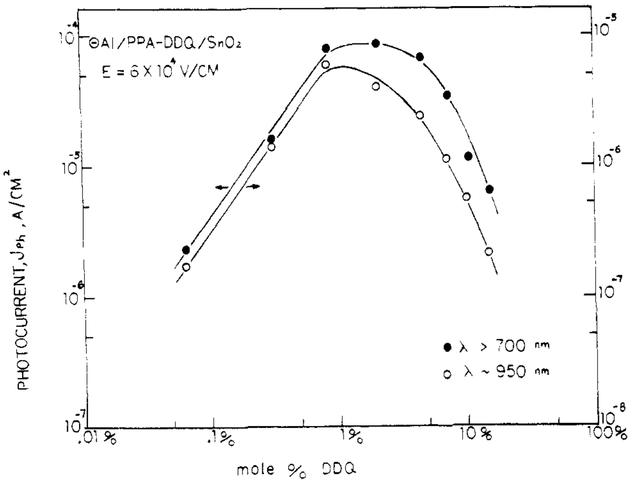

Figure 5. Photocurrent density vs. doping level in PPA-DDQ.

for the undoped polymer as the exciting wavelengths are changed from λ >700 to λ >510 nm, whereas a slope of 0.5 is approached in the doped polymers. This value indicates an equilibrium between conduction electrons and shallow traps in undoped PPA and an equilibrium between free carriers trapped on the charge-transfer complex in the doped polymers (see Discussion).

The field (E) dependence of J_{ph} is shown as a log-log plot in Figure 7. All slopes are greater than 1, an indication of space charge-perturbed photocurrents, associated with a large population of trapped charge.[14]

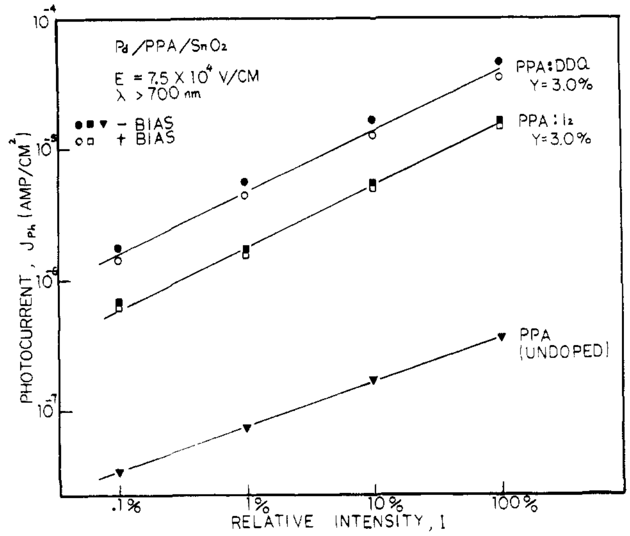

Figure 6. Photocurrent density vs. light intensity in various samples.

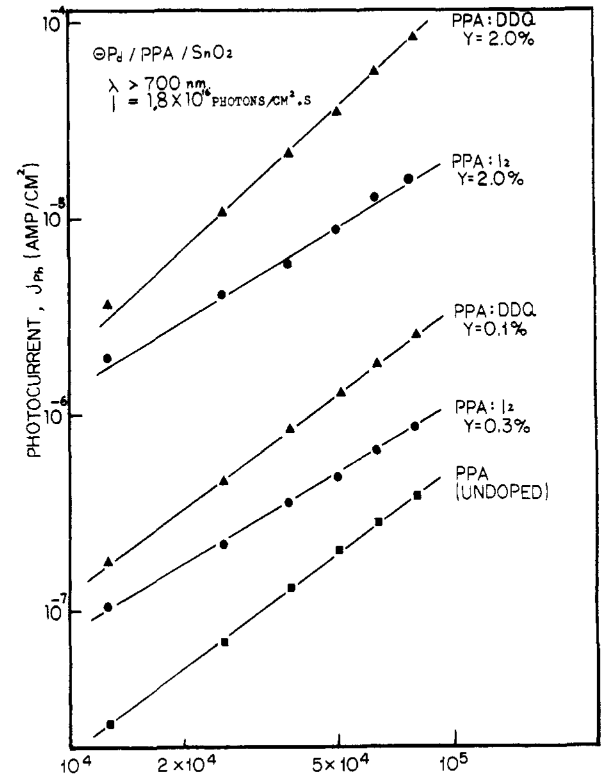

Figure 7. Photocurrent density vs. electric field in various samples.

The possibility was explored of obtaining information on carrier lifetimes and mobilities from pulsed photoconductivity data. The experiment was successful for PPA-DDQ, where the mobilities were sufficient for the transit time, t_T, to be shorter than the lifetime for electrons, τ_n, and where both just exceeded the pulse width of the source, which was about 3 μs. In PPA-I_2 only lifetime measurements were successful. The current pulses in Al/PPA-DDQ/SnO_2 with the top electrode biased positively and negatively are shown in parts a and b of Figure 8, respectively. In both cases, the system RC time constants are less than the carrier transit times and the pulse decay constants. A knee in the plot, marking t_T, is visible for electrons (positive bias on Al, with light impinging on the transparent SnO_2 electrode) but not for holes. Lifetimes of 6.5 μs for electrons and of 4 μs for holes are obtained from the pulse decay times. μ_n is calculated to be 2×10^{-3} cm²/(V·s). We also note the absence of a long tail that is often present in amorphous photoconductors, including poly(vinylcarbazole) (PVK).[15]

Electron mobilities can be also calculated for the undoped polymer and are much smaller. This can be accomplished by determining the time integral of the detrapping currents, $\int_0^\infty i \, dt$, where i is the time-dependent current obtained when a light flash, in the absence of the electric field, is directed at a sample having undergone a steady-state photoconductivity experiment,[1] so that all the traps may be assumed to be occupied. The integral rep-

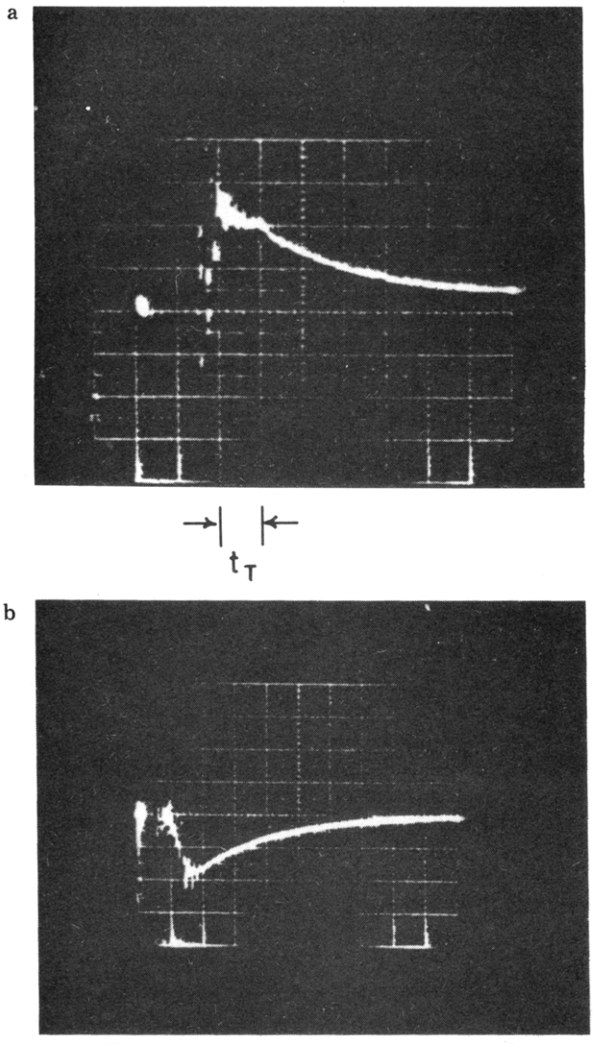

Figure 8. Traces of photocurrent decay in PPA–DDQ, $Y = 2.0\%$, following a 3-μs flash. (a) Transient electron current, $R = 2.2$ kΩ, $V = 30$ V, x-axis = 2 μs/div, y-axis = 0.1 V/div. (b) Transient hole current, $R = 4.7$ kΩ, $V = 30$ V, x-axis = 2 μs/div, y-axis = 0.5 V/div.

resents the charge of the trapped electrons from which one can calculate the concentration of the shallow electron traps,[1] which may be equated to the steady-state concentration of the negative charge carriers. An electron mobility of 2×10^{-7} cm^2/(V·s) is then obtained from the magnitude of the steady-state photocurrent, assuming it to be made up entirely of electrons.[16,17]

Discussion

We wish to propose a mechanism for photoconductivity in PPA and its charge-transfer complexes. The deep trapping of holes in undoped PPA, leading to the presence of nearly unipolar dark currents and photocurrents in sandwich arrangements with one injecting and one blocking electrode, facilitates the analysis and permits a good estimate of the concentration of shallow electron traps at 10^{13}–10^{16} cm^{-3} from an analysis of the detrapping currents.[17] The presence of shallow electron traps which can be depopulated by low-energy radiation implies the existence of more mobile states for electron transport through the sample and suggests the applicability of a band model. The electron mobility of 2×10^{-3} cm^2/(V·s) in PPA–DDQ, which is known to be trap modulated, yet greater than the highest values reported for PVK,[18] is still too low to be offered as evidence that extended states participate in the transport process; however, the short carrier lifetimes which are associated with the prominence of bulk recombination processes, and hence an equilibrium between mobile and immobile states, do lend support to a band model. We also note the absence of a long tail in the photocurrent pulses which, in the Scher–Montroll model,[19] is indicative of a highly dispersive non-Gaussian transport mechanism between localized, isoenergetic states. Finally, the existence of a photocurrent maximum at an optimum doping level is characteristic of a semiconducting photoconductor having a band structure.[20] These factors then suggest a mechanism that might be described as "trap-modulated bandlike transport". We must emphasize at this point that we have found no evidence for transport through extended states in dark conductivity.[6,7]

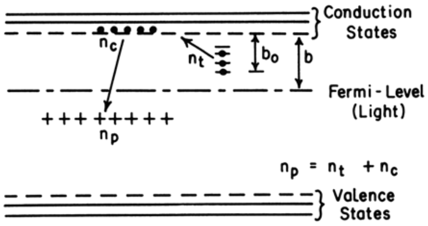

Figure 9. Band model for undoped PPA: n_c = electrons in mobile states; n_t = electrons in shallow traps; n_p = holes in deep traps. Dashed lines indicate a diffuse band edge or mobility edge.

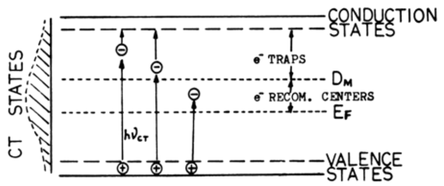

Figure 10. Photocarrier generation and recombination in PPA doped with a charge-transfer (CT) complex.

In the undoped polymer, electrons are injected from the electrode into defect states lying in the band gap; these electrons then equilibrate with the conduction states in the presence of light, and recombination takes place with the fixed holes, which are inferred from the presence of near unipolar electron currents. The promotion of electrons from shallow traps into conducting states is a photodetrapping process, which appears to control the photoconductivity under most conditions described; as the wavelength is increased, the intensity exponent of J_{ph} falls progressively below 0.5,[1] suggesting that thermal processes make a progressively greater contribution to detrapping as emptiable traps become shallower. In doped PPA, in which the charge-transfer complex has been shown to be the main source of the photocarriers (Figures 4 and 5), that complex introduces a new set of traps and recombination centers possessing a range of energies that lie in the band gap of the undoped polymer.

These considerations suggest that band models for undoped PPA and for PPA–I$_2$ or PPA–DDQ can be adapted from a set proposed by Rose.[14] They are shown in Figures 9 and 10. n_c represents conduction electrons, n_t electrons in shallow traps, and n_p deeply trapped holes. E_F represents the Fermi level and D_M the demarcation level which separates shallow traps, from which electrons can be returned to the conduction band, from deep, permanent traps.[20] It can be shown that upon acceptor doping E_F can shift toward the valence band, while D_m moves toward the conduction band, turning some shallow traps into deep traps.[20] This causes an optimum doping level for maximum sensitization by the dopant, as seen in PPA–DDQ (Figure 5). The large positive temperature coefficient of J_{ph} for undoped PPA observed just above room temperature,[9] together with the half-power dependence on the light intensity, which is approached at the shorter wavelengths, is consistent with a distribution of shallow traps above the Fermi level.[14] In the doped polymer, the half-power dependence of J_{ph} on the light intensity arises from the pairwise recombination of electrons and holes originating from the charge-transfer complex.

Some comments may be appropriate on charge carrier generation in the undoped polymer, in which carriers must be injected from the negative electrode into defect states lying in the band gap of the polymer; these electrons then must enter the conduction states by photon or thermal activation, as already discussed. Such defect states make a positive contribution to the photocurrent, as is indicated by the positive correlation between detrapping currents and steady photocurrents at low trap concentrations.[17] It seems premature to speculate about details of the injection process, since the band alignment at the metal/PPA interface is still unknown. On the basis of a band gap of 2.3 eV,[21] an ionization potential of 4.9 eV was calculated from the junction potential in PPA–AsF_5, assuming the Fermi level of the metal lines up with the valence band edge of the heavily doped polymer.[5] The location of the charge-transfer band in PPA–I_2 and PPA–DDQ suggests, however, that the ionization potential of the undoped polymer is in the range of 5.5–5.7 eV.[3] Such a value, which would account for the oxidative stability of the polymer, would also place the Fermi level of the injecting electrode near the middle of the band gap of the polymer.

A bandlike model is also supported by experiments of PPA doped with the dyes pyronin Y or methylene blue,[23] which should be capable of injecting electrons directly into the conduction band of PPA from their excited states.[23] Each dye enhances the photoconductivity in its absorption band, while the diffusion-limited Schottky–Richardson voltage dependence of the dark current ($j_d \propto V^{3/2}$), which is typical for undoped PPA,[1] changes to an ohmic dependence; also, the exponent of the intensity dependence of J_{ph} changes to 1.0. These effects indicate that defect states no longer control the injection process, as they do in undoped PPA, nor is there a trap-controlled generation–recombination equilibrium mediated by the charge-transfer complex as in PPA–I_2 and PPA–DDQ. Thus, direct injection into the conduction band of the polymer, rather than into defect states lying in the band gap, results in behavior more typical of organic solids with a recognized band mechanism.[20]

The results of this study indicate that PPA and its charge-transfer complexes are semiconducting photoconductors with a phototransport mechanism significantly different from the hopping transport that occurs in the insulating polymer PVK and its charge-transfer complexes[25] and which, in many respects, resembles that in low molecular weight organic solids and inorganic semiconductors. The strongly unipolar, trap-modulated electron transport in undoped PPA, which depends strongly on the microstructure of the polymer, might be a characteristic of near-planar trans polyene chains. In polyacetylene, as in PPA, significant photoconductivity was observed in the trans isomer and not the cis isomer, but the phenomenon was interpreted in terms of the soliton model.[26]

Acknowledgment. We express our thanks for the *trans*-PPA samples to Professor T. Higashimura and Dr. T. Masuda, Kyoto University, and to the Polymers Program, National Science Foundation, for support of this research.

Registry No. Poly(phenylacetylene) (homopolymer), 25038-69-1; 2,3-dichloro-5,6-dicyano-*p*-benzoquinone, 84-58-2; iodine, 7553-56-2.

References and Notes

(1) E. T. Kang, P. Ehrlich, A. P. Bhatt, and W. A. Anderson, *Appl. Phys. Lett.*, 41, 1136 (1982).
(2) E. T. Kang, P. Ehrlich, A. P. Bhatt, and W. A. Anderson, *Polym. Prepr., Am. Chem. Soc., Div. Polym. Chem.*, 24(2), 73 (1983).
(3) E. T. Kang, Ph.D. Thesis, SUNY—Buffalo, 1983.
(4) T. Masuda, Y. Kuwane, K. Yamamoto, and T. Higashimura, *Polym. Bull. (Berlin)*, **2**, 823 (1980).
(5) E. T. Kang, A. P. Bhatt, E. Villaroel, W. A. Anderson, and P. Ehrlich, *J. Polym. Sci., Polym. Lett. Ed.*, **20**, 143 (1982).
(6) A. P. Bhatt, E. T. Kang, W. A. Anderson, and P. Ehrlich, *J. Appl. Phys.*, **54**, 3973 (1983).
(7) A. P. Bhatt, W. A. Anderson, and P. Ehrlich, *Solid State Commun.*, **47**, 997 (1983).
(8) T. J. Sanford, R. D. Allendoerfer, E. T. Kang, and P. Ehrlich, *J. Polym. Sci., Polym. Phys. Ed.*, 18, 2277 (1980).
(9) E. T. Kang, unpublished results.
(10) Y. Kuwane, T. Masuda, T. T. Higashimura, *Polym. J.*, 12, 387 (1980).
(11) P. Cukor, J. I. Krugler, and M. F. Rubner, *Makromol. Chem.*, **1982**, 165 (1981).
(12) E. T. Kang, S. H. Lee, P. Ehrlich, and W. A. Anderson, *Bull. Am. Phys. Soc.*, **29**, 560 (1984).
(13) J. Kanicki, E. Vander Donckt, and S. Boué, *J. Chem. Soc., Faraday Trans. 2*, 77, 2157 (1981); *Thin Solid Films* **92**, 243 (1982).
(14) A. Rose, "Concepts in Photoconductivity and Allied Problems", Robert E. Krieger Publishing Co., Huntington, NY, 1978.
(15) R. C. Hughes, in "Photoconductivity in Polymers", A. V. Patsis and D. A. Seanor, Ed., Technomic Publishing Co., Westport, CT, 1976, p 158.
(16) Reference 1, Figure 1.
(17) Reference 1, Figure 3.
(18) R. C. Hughes, *Appl. Phys. Lett.*, **21**, 196 (1972); A. Szymanski and M. M. Labes, *J. Chem. Phys.*, **50**, 3568 (1969).
(19) H. Scher and E. W. Montroll, *Phys. Rev. B*, **12**, 2455 (1975).
(20) H. Meier, "Organic Semiconductors", Verlag Chemie, Weinheim, 1974, Chapter 3.
(21) D. Bloor, *Chem. Phys. Lett.*, **43**, 270 (1976).
(22) T. Masuda, N. Sasaki and T. Higashimura, *Macromolecules*, 8, 717 (1975).
(23) E. T. Kang, P. Ehrlich, and W. A. Anderson, *Mol. Cryst. Liq. Cryst.*, **106**, 305 (1984).
(24) Reference 20, p 154.
(25) J. M. Pearson and M. Stolka, "Poly(N-Vinylcarbazole)", Gordon and Breach, New York, 1981, Chapter 4.
(26) L. Lauchlan, S. Etemad, T. C. Chung, A. J. Heeger, and A. G. MacDiarmid, *Phys. Rev. B*, **24**, 3701 (1981).